Proteoglycan (PG)-induced arthritis (PGIA) and recombinant human PG-G1 domain-induced arthritis (GIA) in BALB/c mice resembling two subtypes of rheumatoid arthritis

Tibor T. Glant, **Marianna Radacs**, **Gyorgy Nagyeri**, **Katalin Olasz**, **Anna Laszlo**, **Ferenc Boldizsar**, **Akos Hegyi**, **Alison Finnegan**, and **Katalin Mikecz**
Section of Molecular Medicine, Departments of Orthopedic Surgery, Biochemistry, Internal Medicine (Section of Rheumatology) and Department of Immunology/Microbiology, Rush University Medical Center, Chicago, IL-60612, USA

Tibor T. Glant: Tibor_Glant@rsh.net; Marianna Radacs: radacs@jgypk.u-szeged.hu; Gyorgy Nagyeri: gyorgynagyeri@yahoo.com; Katalin Olasz: katalin.olasz@gmail.com; Anna Laszlo: alaszlo@calculus.hu; Ferenc Boldizsar: fboldizsar@gmail.com; Akos Hegyi: hegyiakos@hotmail.com; Alison Finnegan: Alison_Finnegan@rsh.net; Katalin Mikecz: Katalin_Mikecz@rsh.net

Abstract

Objective—To develop a simplified and relatively inexpensive version of the cartilage proteoglycan (PG)-induced arthritis (PGIA), an autoimmune model of rheumatoid arthritis (RA); and to evaluate the extent to which this new model replicates the disease parameters of PGIA and RA.

Methods—Recombinant G1 domain (rhG1) of human cartilage PG containing "arthritogenic" T-cell epitopes was generated in a mammalian expression system and used for immunization of BALB/c mice. The development and progression of arthritis in rhG1-immunized mice (designated rhG1-induced arthritis, GIA) was monitored, and disease parameters were compared to those in the parent PGIA model.

Results—GIA highly resembles PGIA, though the clinical symptoms and immune responses in mice with GIA are more uniform than in those with PGIA. Mice with GIA showed evidence of stronger T-helper 1 (Th1) and 17 (Th17) polarization than those with PGIA, and anti-mouse PG autoantibodies were produced in different isotype ratios in the two models. RF and anti-cyclic citrullinated peptide (anti-CCP) antibodies were detected in both models; however, serum levels of IgG-RF and anti-CCP antibodies were different in GIA and PGIA, and both parameters correlated better with disease severity in GIA than in PGIA.

Correspondence and reprint request address: Tibor T. Glant, MD, PhD, Section of Molecular Medicine, Department of Orthopedic Surgery, 1735 W. Harrison St., Cohn Research Building, Room 708, Chicago, IL, 60612 Phone: 312-942-9733; Fax: 312-942-8828; Tibor_Glant@rsh.net.
Tibor T. Glant; Alison Finnegan; Katalin Mikecz; Gyorgy Nagyeri; Akos Hegyi - Rush University Medical Center, Chicago, IL, USA; Marianna Radacs[1] - Gyula Juhasz Faculty of Education, University of Szeged, Szeged, Hungay
Ferenc Boldizsar and Katalin Olasz - Department of Immunology and Biotechnology, University of Pecs, Pecs, 7643, Hungary
Anna Laszlo, Calculus Ltd., Hungary

Conclusion—GIA is a novel seropositive model of RA, exhibiting all of the characteristics of PGIA. Although the clinical phenotypes are similar, GIA and PGIA are characterized by different autoantibody profiles and the two models may represent two subtypes of seropositive RA, where more than one type of autoantibodies can be used to monitor disease severity and response to treatment.

Keywords

autoimmunity; arthritis; PGIA; GIA; RF; anti-CCP antibody

INTRODUCTION

Rheumatoid arthritis (RA) is an autoimmune disease in which chronic inflammation of the synovial joints leads to cartilage destruction and bone erosion. Although the etiology of RA is unknown, both environmental and genetic factors are thought to be involved in the pathogenesis of the disease (1). Animal models of arthritis, particularly those that allow for investigation of joint pathology in genetically susceptible rodents (2), are invaluable tools for RA-related research. Among the systemic animal models of RA, human cartilage proteoglycan (PG aggrecan)-induced arthritis (PGIA) in BALB/c mice is a T cell-dependent and (auto)antibody/B cell-driven disease (3–5). In addition to the major histocompatibility complex (MHC), PGIA is controlled by multiple genetic loci (5), many of which are located in chromosomal regions that are analogous to human regions identified in genome-wide association studies of RA (6,7).

The BALB/c mouse strain is genetically predisposed to the development of arthritis. In addition to PG (aggrecan), immunization with human cartilage link protein (8) or cartilage glycoprotein-39 (HC-gp39) (9), but not type II collagen (10,11) induces arthritis in BALB/c mice. The BALB/c strain is highly susceptible to serum-transfer arthritis induced by injection of serum from arthritic K/BxN mice (12,13), and this strain also develops arthritis in response to streptococcal cell-wall injection (14). Moreover, interleukin-1 (IL-1) receptor antagonist protein-deficient mice (15) and SKG mice that carry a point mutation in the gene encoding ZAP-70 both develop spontaneous arthritis (16), though this only occurs in mice with a BALB/c background.

Several years ago, we "simplified" the PGIA model by replacing purified human fetal cartilage PG (3,4) with PG isolated from human osteoarthritic cartilage (11,17) and Freund's adjuvant with a synthetic adjuvant (18); this simplification allowed us to use the model for more extensive studies, including genome-wide screening of arthritis-associated chromosomal regions (5). However, the source of antigen (human cartilage) and the cost of antigen preparation were still limiting factors in the wide-range application of the PGIA model. More recently, we mapped the T-cell epitope repertoire of the core protein of human PG (aggrecan) in BALB/c mice and found that three arthritogenic/dominant and four subdominant T-cell epitopes were located in the G1 domain of PG (19–21). Immunization of BALB/c mice with short synthetic peptides corresponding to these epitopes (either alone or in combination) failed to induce arthritis, prompting us to generate a recombinant human (rh)G1 domain that contained all of the dominant and sub-dominant T-cell epitopes. Unfortunately, when expressed in prokaryotic cells, the non-glycosylated G1 domain was completely insoluble. The use of a baculovirus expression system seemed to be a more promising approach (22,23), though difficulties with the virus titration and antigen purification procedures precluded the generation of large quantities of G1 protein. Finally, using a mammalian expression system, we succeeded in a large-scale production of rhG1-recombinant mouse (rm)IgG-Fc fusion protein containing enzymatic cleavage site(s) for easy purification.

Here, we describe a new, improved PGIA model that is induced by immunization of BALB/c mice with the rhG1 domain of cartilage PG, thus, we have designated this new model GIA (G1 domain-induced arthritis). We used both the rhG1-rmIgG-Fc fusion protein and purified rhG1 (without rmIgG-Fc partner) to induce GIA in BALB/c mice, and we then compared this model with the "parent" PGIA model. The GIA model exhibits all of the characteristics described so far for systemic autoimmune arthritis models. Although we did not expect GIA to be more robust than PGIA, side-by-side comparisons revealed that mice with GIA developed arthritis more uniformly and with higher overall inflammation scores than those with PGIA. We found that both GIA and PGIA were associated with abundant production of autoantibodies (autoAbs) to mouse (self) PG. However, the two models could be distinguished on the basis of "RA-specific" serological markers. Mice with GIA produced higher quantities of rheumatoid factor (RF) than those with PGIA, whereas mice with PGIA had significantly higher serum levels of anti-citrullinated peptide (anti-CCP) Abs (or ACPA) than mice with GIA.

MATERIALS AND METHODS

Generation of a recombinant G1 fusion protein

A cDNA fragment (753 base pairs long) of the mouse IgG2a heavy chain was obtained by reverse transcription of RNA purified from a monoclonal Ab (mAb)-producing B-cell hybridoma. The cDNA fragment was amplified by polymerase chain reaction (PCR) using primers with linkers for restriction enzyme (*Eco*RI and *Bcl*I) cleavage sites. The cDNA included the hinge region of the heavy chain, and was inserted into a Lonza pEE14.1 mammalian expression vector (Lonza Biologics Ltd, Slough, UK). Total RNA was extracted from human chondrocytes using TriReagent, reverse transcribed and amplified by PCR. Subsequently, the cDNA fragments (with *Eco*RI sites) coding for the 351 amino acid-long G1 domain and 59 amino acids of the interglobular domain (IGD) of PG (23) were cloned into a pBlueScript S/K vector (Stratagene, La Jolla, CA) (Figures 1A, B and C). The 5′-end of the IGD region was mutated to carry the cleavage site for endopeptidase Factor Xa, and the construct was inserted into the *Eco*RI site in frame with the mFc2a-Lonza construct (Figure 1C). Appropriate orientation was determined by PCR, and the entire construct was sequenced. The IGD included the natural cleavage sites for stromelysin (MMP3) and two aggrecanases (ADAMTS-4 and -5) as well as the Xa cleavage site that was inserted between the IGD and the heavy chain of mouse IgG2a (Figure 1D).

Semi-confluent CHO-K1 (Chinese hamster ovary) cells were transfected with the hG1-Xa-mFc2a Lonza construct using a $CaCl_2$ precipitation method followed by positive selection according to the manufacturer's protocol. First-step (i.e., cloning directly from Petri dishes) and second-step (i.e., repeated cloning by limiting dilution) cloning procedures were performed in Ultra-CHO serum-free medium (CHO-SFM, Lonza BioWhittaker, Walkersville, MD). Irradiated mouse embryonic fibroblasts were used as feeder cells. G1 expressing clones were identified by incubating CHO-SFM supernatant-coated plates with biotinylated mAb G18, followed by detection using peroxidase labeled streptavidin and tetramethyl-benzidine substrate (BD Biosciences, San Diego, CA). The mAb G18 (IgG1) is specific for an epitope in the A-loop of the G1 domain (Figures 1A and B) of human PG (aggrecan) and does not cross-react with mouse PG (11,23). Alternative wells were tested with anti-mouse IgG2a, and the highest G1-expressing clones were selected. The rhG1-Xa-mFc2a fusion protein was purified from CHO-SFM using Protein G-Sepharose 4B (Pierce, Rockford, IL). The yield of the rhG1-Xa-mFc fusion protein was approximately 8–10 mg per liter of CHO-SFM. The expression level, quality of purification, and amounts of the G1 domain expressed (relative to the amounts of native G1 domain isolated from human PG) were determined by sodium-dodecyl sulphate polyacrylamide gel electrophoresis (SDS-PAGE) and western blotting analysis using mAb G18. Purified rhG1-Xa-mFc2a fusion

protein was cleaved with Factor Xa (1,000 units per 10 mg fusion protein) (Novagen, Madison, WI). The enzyme was removed by incubation with Xarrest Sepharose (Novagen), and the IgG2a-Fc fragment was absorbed to Protein-G Sepharose. The type and level of glycosylation of purified rhG1 was determined using a deglycosylation kit (QA-Bio LLC, Palm Desert, CA) according to the manufacturer's instructions.

Immunization of BALB/c mice with cartilage PG or rhG1

Cartilage from knee joints was obtained from consenting osteoarthritis patients who had undergone joint replacement surgery. The use of human cartilage for PG isolation was approved by the Institutional Review Board of Rush University Medical Center (Chicago, IL). The PG isolation and deglycosylation procedures have been described in detail in previous studies (11,17). Female BALB/c mice (16–24 weeks of age) were purchased from the National Cancer Institute, Frederick, MD. All animal experiments were approved by the Institutional Animal Care and Use Committee of Rush University Medical Center.

For immunization with PG, 100 μg of PG core protein was emulsified with 2 mg dimethyl-dioctadecyl ammoniumbromide (DDA) adjuvant in phosphate buffered saline (PBS, pH 7.4) following a standard procedure (11). After titration of the optimal dose, 40 μg of rhG1 domain (or rhG1-Xa-mFc2a fusion protein equivalent to 40 μg of purified rhG1) was emulsified using 2 mg of DDA in PBS (in a total volume of 300 μl) and injected intraperitoneally (i.p.) on days 0, 21, and 42 for induction of GIA (18). Mice injected with 2 mg of DDA in 300 μl PBS or CHO-SFM were used as negative controls.

Clinical and histological assessment of arthritis

Arthritis severity was determined using a visual scoring system based on the degree of swelling and redness of the front and hind paws (3,4,11). Animals were examined at least three times a week; the degree of inflammation was scored from 0 to 4 for each paw, resulting in a cumulative arthritis score ranging from 0 to 16 for each animal (3,11). All mice were scored by two different investigators in a blinded manner. The incidence of arthritis was expressed as the percentage of immunized mice that were arthritic. Upon sacrifice, limbs were removed, fixed in 10% formalin, acid decalcified, embedded in paraffin, and processed according to standard histological procedures (3,5,11,24).

Measurement of antigen-specific T-cell responses and serum levels of cytokines and anti-PG antibodies

Antigen-specific lymphocyte responses were determined in spleen cell cultures in the presence or absence of 50 μg/ml human PG or 10 μg/ml rhG1 domain. Cells were cultured in HL-1 serum-free medium (BioWhittaker/Lonza, Walkersville, MD) for 2 days, and antigen-specific IL-2 production was measured using the CTLL-2 bioassay (3,4,11). Cell proliferation was assessed on the fifth day of culture by measuring [^{3}H]-thymidine incorporation (4,11), and antigen-specific proliferation of spleen T-cells was expressed as a stimulation index (3,4,11). The serum cytokines IL-1β, IL-4, IL-6, IL-17, IFN-γ and TNF-α were measured using ELISA kits purchased from R&D Systems (Minneapolis, MN) or BD Biosciences (San Diego, CA). *In vitro* production of these cytokines was also assessed by measuring their concentrations in supernatants of antigen (PG or rhG1)-stimulated spleen cell cultures on the fifth day of culture using ELISA. Cytokine concentrations were normalized to cell number (pg or ng of cytokine per million spleen cells), as described previously (5,25).

PG-specific serum antibodies (Abs) were quantified by ELISA using serially diluted serum samples. Purified human or mouse cartilage PG, or rhG1 without the Fc tail were immobilized in Maxisorp 96-well plates (Nunc International) at a concentration of 0.1 μg/

well each (11). For PG-specific IgG isotype assays, peroxidase-labeled goat anti-mouse IgG1 Ab (Zymed Laboratories, San Francisco, CA) or IgG2a (BD Biosciences) was used after incubation with serum. Serum PG-specific antibody levels were calculated using serial dilutions of pooled sera of mice with PGIA and known antibody titers (11).

Measurement of RF and anti-CCP Abs in serum

Mouse IgG- and IgM-type RFs were measured in mouse IgG2a-Fc coated plates; the IgG2a-Fc fragment was isolated from the mTSG6-Xa-mFc2a fusion protein after cleavage with factor Xa and purification on Protein G. RFs (mouse Fc-binding autoAbs) were measured in serially diluted (1:500–1:2,000 for IgM-RF and 1:2,000–1:8,000 for IgG-RF) serum samples collected at different time points of immunization. Fc-bound IgG-type and IgM-type RFs were detected using polyclonal Abs to mouse IgG1 and IgM (γ1- and μ-chain-specific, respectively). The results were validated (units/ml serum) by re-testing representative samples using commercially available mouse IgG-RF and mouse IgM-RF ELISA kits (Shibayagi Co., Shibukawa, Japan).

Anti-CCP (cyclic citrullinated peptide) antibody levels were quantified using Quanta Lite[TM] CCP-3 ELISA kits (Inova Diagnostics Inc., San Diego, CA) with a minor modification to the manufacturer's protocol to detect mouse anti-CCP Abs. In brief, serially diluted serum (previously pooled from mice with PGIA) was titrated to correspond to the highest arbitrary ("calibrator") unit of the human reference sample in the kit by adjusting the dilution of the peroxidase-labeled secondary (anti-mouse IgGAM) antibody. Our mouse serum with anti-CCP Abs was calibrated to contain 250 arbitrary units/μl serum and was then used as the mouse reference sample/standard in all subsequent experiments.

Statistical analysis

Descriptive statistics were used to determine group means and standard errors of the means (mean ± SEM). Differences between two groups were tested for statistical significance using the Student's *t*-test, and differences between three or more groups were tested for statistical significance by one-way ANOVA followed by the least significant difference post hoc test. Fisher's Exact Chi-square test was used to evaluate statistical significance when disease parameters were compared. All statistical analyses were performed using the SPSS (version 16.0) statistical software package (SPSS, Chicago, IL). A p value of less than 0.05 was considered statistically significant.

RESULTS

Characterization of rhG1 and the clinical phenotype and histopathology of GIA

We developed a mammalian expression system for the large-scale production of the G1 domain of human PG; our goal was to replace the antigen (PG isolated from human cartilage) for the immunization of, and arthritis (GIA) induction in, genetically-susceptible BALB/c mice. Figure 1D shows representative schematics of the rhG1-Xa-mFc2a fusion protein. The Fc tail of the IgG2a heavy chain was properly folded; therefore, the paired heavy chains were able to bind to Protein G. As demonstrated by SDS-PAGE and western blotting analysis using the human G1-specific mAb G18 (Figure 1E), the rhG1-Xa-mFc2a fusion protein was effectively purified from the supernatants of a CHO-K1 transfectant clone. Cleavage of the fusion protein with factor Xa and removal of the Fc tail on Protein G-Sepharose yielded nearly 100% pure rhG1 domain. A reduction in the molecular mass of the purified rhG1 fragment after digestion with various glycosidases indicated that the protein was secreted by the mammalian cells (CHO) in a glycosylated form that contained both *N*-linked and *O*-linked oligosaccharides (Figure 1F).

Purified rhG1-Xa-mFc2a fusion protein that had not been cleaved with Xa was used first for immunization of BALB/c mice that were then compared with the "parent" PGIA model (Figs 2A–B). Approximately 10.0–12.5 μg of purified rhG1 (either fusion protein or single G1 domain) in DDA adjuvant was the lowest threshold dose for the induction of arthritis, while 100 μg or more of rhG1 resulted in an "overdose" that actually delayed the onset of arthritis (data not shown). The optimal dose was found to be between 25 μg and 50 μg of recombinant protein. Therefore, we routinely used 40 μg of rhG1 (emulsified in DDA) per injection. As in the PGIA model, the earliest onset of arthritis (occurring in approximately 10% of all immunized mice) was noted after the second injection (11) and was mostly restricted to the inter-phalangeal and metacarpo- and/or metatarso-phalangeal joints. In a side-by-side comparison, GIA reached 98–100% incidence levels 9–10 d after the third immunization (Figure 2A), and the cumulative arthritis score was consistently higher in the GIA model than the PGIA model (Figure 2B). Overall, the two models were very similar; however, inflammation was initiated more robustly and involvement of the front paws was more extensive in the GIA model. Consistent with this finding, cartilage and bone destruction in the front paws appeared to be more progressive in the GIA model than in the PGIA model, though the clinical symptoms (i.e., redness and swelling of affected joints) were comparable between the two groups. The joints became severely deformed due to the inflammatory destruction of cartilage and bone (Figure 3), similar to results observed in previous investigations of PGIA (3,5,11). At the late, chronic stage of arthritis (2–3 months after onset), there were no clinical or histopathological differences between the two models (results not shown).

T- and B-cell-mediated immune responses in GIA and PGIA

In vitro tests (i.e., T-cell proliferation and cytokine production) showed evidence of robust T-cell responses to rhG1 or PG-stimulation. As expected, the magnitude of the responses to these antigens was different in the two models. Mice immunized with rhG1 exhibited higher levels of T-cell stimulation (expressed as stimulation index) with rhG1 than with PG (Figure 2C, two left-hand graphs), and, vice versa, T cells from PG-immunized mice exhibited higher proliferation and IL-2 production in response to stimulation with PG than with rhG1 (Figure 2C, two right-hand graphs). Antigen-specific production of IL-6, TNF-α, and IL-4 was higher in spleen cell cultures of mice with PGIA than those with GIA, though significantly more IFN-γ and IL-17 were secreted by spleen cells of mice with GIA (Figure 2D). Serum levels of IL-17 and IL-1β were almost two-fold higher in mice with GIA compared to mice with PGIA, though essentially no TNF-α was detected in the sera of arthritic mice immunized with rhG1 (Figure 2E).

Serum levels of Abs to rhG1 or human cartilage PG (especially the IgG1 isotype) were approximately three-four times higher in mice with PGIA than in those immunized with rhG1; this was probably due to the presence of multiple epitopes (including immunogenic carbohydrate stubs) in full-length PG obtained from cartilage (Figure 2F). However, anti-mouse PG autoAb levels exhibited an opposite trend, and unusually high concentrations of anti-mouse PG IgG2a isotype Abs were detected in the sera of mice with GIA (Figure 2F). The IgG2a/IgG1 ratio of anti-mouse PG autoAbs was 4.62 in mice with GIA and 0.75 in mice with PGIA, suggesting a strong Th1 polarization (also indicated by the cytokine profile (Figures 2D and E) in rhG1-immunized mice.

Serum (auto)Ab levels as disease biomarkers of PGIA and GIA

The unusually high serum levels of anti-mouse PG autoAbs (especially of the IgG2a isotype) (Figure 2F) prompted us to investigate whether other arthritis-related ("RA-specific") antibodies, such as RF or anti-CCP antibodies, were also produced in mice with GIA or PGIA. To this end, we collected blood samples every 7–8 days during the

experimental period from mice immunized with rhG1, rhG1-Xa-mFc2a, mFc2a, or human PG. Mice injected with PBS in DDA adjuvant served as negative serum control donors (only results from experiments with rhG1 fusion protein- and human PG-immunized mice are shown). As shown in Figure 4, serum levels of all autoAbs, including anti-mouse PG (IgG1 and IgG2a isotypes) (Figures 4E and F), IgG-type and IgM-type RFs (Figures 4C and D), and anti-CCP Abs (Figure 4B) started to rise weeks before the first appearance of clinical symptoms of arthritis (Figure 4A). While IgM-type RF and IgG2a anti-mouse PG Ab levels were similar in the two models (Figures 4D and F), the levels of IgG1 anti-mouse PG autoAbs and anti-CCP Abs were approximately 4 to 5 times higher in the sera of mice with PGIA than in those with GIA (Figures 4B and E). In contrast, IgG-type RF was the most prominent autoAb in mice with GIA (Figure 4C). The serum levels of these autoAbs (except for IgM-type RF in mice with GIA) showed significant positive correlation with increasing arthritis severity scores (Figure 4A) in both the GIA and PGIA models (data not shown).

We next investigated whether the serum levels of any specific autoAb could "predict" the onset time or severity of arthritis in individual animals with either GIA or PGIA. Because all rhG1- and human PG-immunized mice developed arthritis by the end of this experiment, we selected the lowest (late onset, low severity) and highest responder mice from each group and compared their arthritis onset time and severity scores with their serum autoAb levels over time (Figures 4G–J). The levels of all autoAbs rose quickly in the serum of the high-responder mice from both the GIA and PGIA groups, and we did not observe any difference between the two models (Figures 4H and J). However, low serum levels of IgG-RF and anti-CCP Abs were associated with the low-responder mouse (delayed onset and low disease severity) from the GIA group (Figure 4G) but not the low-responder from the PGIA group (Figure 4I).

DISCUSSION

In this study, we have described GIA, a simplified and improved version of cartilage PG-induced arthritis (PGIA) (3,5). GIA was induced by systemic immunization of female BALB/c mice with a recombinant protein (G1 domain of human PG) in synthetic DDA adjuvant, and the parameters of arthritis in these animals were compared to those with PGIA. The incidence of arthritis reached 95–100% in both GIA and PGIA, though disease severity was consistently higher in the GIA model than in the parental PGIA model, primarily due to a more extensive involvement of the front paws in the inflammatory process. However, joints commonly affected in both models (e.g., the ankle) did not show significant macroscopic or microscopic differences at the peak of arthritis. As expected, T cells from mice with GIA reacted better (in terms of proliferation and IL-2 production) to in vitro stimulation with rhG1 than with PG; likewise, T cells from mice with PGIA responded more robustly to stimulation with PG than with rhG1. However, both models showed evidence of PG-specific autoimmunity, as they produced autoAbs to mouse PG in comparable quantities. We found that there were differences in the production levels of some disease-associated cytokines and Abs between PGIA and GIA. For example, higher serum levels of IL-1β and IL-17, IgG-type RF, and higher IgG2a/IgG1 ratio of autoAbs to mouse PG but lower amounts of anti-CCP Abs were detected in GIA than in PGIA.

Spleen cells from mice with GIA that were stimulated in vitro with rhG1 produced larger quantities of IFN-γ and IL-17, but less TNF-α than PG-stimulated splenocytes from mice with PGIA. PGIA has been postulated to be a Th1-type disease (26–29), with significant IL-17 production (30), where IFN-γ determines the requirement for IL-17 (29). Because the production of both IFN-γ and IL-17 were more robust in GIA than in PGIA, GIA could represent an intermediate form of the disease between the Th1- and Th17-mediated forms. In addition, the propensity of T-cells in mice immunized with rhG1 to produce higher

amounts of IFN-γ and IL-17 than T-cells in PG-immunized animals could contribute to the development of a slightly more severe form of arthritis in mice with GIA. PGIA and GIA are closely related, though they could be distinguished on the basis of select clinical and immunological parameters. Therefore, these models may resemble two sub-types of seropositive RA with slightly different disease phenotypes and cytokine/autoAb profiles. while keeping the scientific direction as close as possible to the human system. However, RA is a heterogeneous disease, and while the various animal models are tremendously helpful for investigating certain aspects of the human disease, none of these models embodies the full spectrum of diseases collectively called RA. Notably, thousands of investigators and pharmaceutical companies use animal models of RA perhaps without understanding the differences among the different subtypes and forms of this disease and the corresponding animal models (2,31–33). Moreover, while animal experiments represent accelerated forms of the disease, RA develops insidiously for decades, and only a few serum markers are indicative of imminent disease.

GIA represents a simplified, uniform, and affordable version of the murine PGIA model. The rhG1 domain contains arthritogenic T-cell epitopes (20) and lacks the undesirable variability of the epitope repertoire that might be found in different preparations of human cartilage-derived PG. GIA exhibits most of the disease characteristics of the parental PGIA model and is now available for laboratories that do not have access to human cartilage or lack experience in PG preparation. The homogeneity of the antigen and the presence of arthritogenic epitopes in rhG1 would also allow for sophisticated in vivo studies on the involvement of autoreactive T-cells (Th subsets) in the disease process. Immunization with a protein that contains multiple T-cell epitopes of the PG molecule, such as rhG1, is necessary for the investigation of disease-related alterations in T-cell function.

An additional value of GIA is the presence of large quantities of IgG-type RF in the circulation (at levels higher than those observed in PGIA) that are absent in commonly used autoimmune models of RA such as murine collagen-induced arthritis (CIA) in DBA/1 strain, or the K/BxN transgenic model of spontaneous arthritis (2). As far as we know, anti-immunoglobulin (RF) and anti-CCP antibodies were observed only in humanized HLA-transgenic mice immunized with type II collagen (34–36), and auto-Abs to citrullinated fillagrin in another study of CIA (37). The prominence of RF and anti-CCP Abs in RA raises the possibility that these Abs play a role in the pathogenesis of the disease. Indeed, Abs with RF activity have been found deposited on the cartilage surface in patients with RA (38,39). AutoAbs in the CIA model or K/BxN transgenic mice have been shown to be pathogenic, as passive transfer of serum from these mice has been shown to induce transient arthritis in naïve recipients (40,41). However, the characteristic autoAbs in these models (against mouse type II collagen and glucose-6-phosphate isomerase, respectively) are detected only in a very small proportion of RA patients (2). Conversely, RF, a characteristic and abundant RA autoAb, is conspicuously absent in CIA and K/BxN mice (2,41); however, anti-CCP Ab injection has been shown to increase the severity of CIA (42). The production of high amounts of RF in GIA would make this model suitable for in vivo studies investigating the emergence of RF-secreting B-cells and potential formation of RF deposits in the joints in the context of arthritis induction.

GIA and PGIA also appear to be the first animal models in which both RF and anti-CCP Abs are detected in the serum. Moreover, serum levels of RF and anti-CCP Abs significantly correlate with arthritis scores and may predict disease severity in individual mice with GIA. Together, RF and anti-CCP Abs are considered important diagnostic/prognostic biomarkers of RA (43–46). Therefore, the presence and prognostic potential of both of these markers in mice with GIA should increase the relevance of this model to RA and its usefulness in pre-clinical studies monitoring the efficacy of emerging drugs in cases of established arthritis.

Acknowledgments

List of abbreviations

|	
Ab	antibody
Abs (or ACPA)	anti-citrullinated peptide (anti-CCP)
CIA	collagen-induced arthritis
CHO-SFM	Ultra-CHO serum-free medium
GIA	G1 domain of cartilage proteoglycan (PG)-induced arthritis
IFN-γ	interferon-γ
IL-	interleukin
mAb	monoclonal Ab
PBS	phosphate-buffered saline (ph 7.4)
PG	cartilage proteoglycan aggrecan
PGIA	PG-induced arthritis
RA	rheumatoid arthritis
RF	rheumatoid factor
rhG1	recombinant human G1 domain of cartilage PG
TCR-Tg	5/4E8 epitope-specific T cell receptor (TCR) transgenic mouse
TNF-α	tumor necrosis factor-α

References

1. Gregersen PK. Genetics of rheumatoid arthritis: confronting complexity. Arthritis Res. 1999; 1:37–44. [PubMed: 11094412]

2. Bevaart L, Vervoordeldonk MJ, Tak PP. Evaluation of therapeutic targets in animal models of arthritis: How does it relate to rheumatoid arthritis? Arthritis Rheum. 2010; 62:2192–205. [PubMed: 20506322]

3. Glant TT, Mikecz K, Arzoumanian A, Poole AR. Proteoglycan-induced arthritis in BALB/c mice. Clinical features and histopathology. Arthritis Rheum. 1987; 30:201–12. [PubMed: 3827960]

4. Mikecz K, Glant TT, Poole AR. Immunity to cartilage proteoglycans in BALB/c mice with progressive polyarthritis and ankylosing spondylitis induced by injection of human cartilage proteoglycan. Arthritis Rheum. 1987; 30:306–18. [PubMed: 3566822]

5. Glant TT, Finnegan A, Mikecz K. Proteoglycan-induced arthritis: immune regulation, cellular mechanisms and genetics. Crit Rev Immunol. 2003; 23:199–250. [PubMed: 14584879]

6. Etzel CJ, Chen WV, Shepard N, Jawaheer D, Cornelis F, Seldin MF, et al. Genome-wide meta-analysis for rheumatoid arthritis. Hum Genet. 2006; 119:634–41. [PubMed: 16612613]

7. Choi SJ, Rho YH, Ji JD, Song GG, Lee YH. Genome scan meta-analysis of rheumatoid arthritis. Rheumatology (Oxford). 2006; 45:166–70. [PubMed: 16278286]

8. Zhang Y, Guerassimov A, Leroux J-Y, Cartman A, Webber C, Lalic R, et al. Induction of arthritis in BALB/c mice by cartilage link protein. Involvement of distinct regions recognized by T- and B lymphocytes. Am J Pathol. 1998; 153:1283–91. [PubMed: 9777960]

9. Verheijden GFM, Rijnders AWM, Bos E, De Roo CJJC, van Staveren CJ, Miltenburg AMM, et al. Human cartilage glycoprotein-39 as a candidate autoantigen in rheumatoid arthritis. Arthritis Rheum. 1997; 40:1115–25. [PubMed: 9182922]

10. Adarichev VA, Valdez JC, Bardos T, Finnegan A, Mikecz K, Glant TT. Combined autoimmune models of arthritis reveal shared and independent qualitative (binary) and quantitative trait loci. J Immunol. 2003; 170:2283–92. [PubMed: 12594249]

11. Glant TT, Mikecz K. Proteoglycan aggrecan-induced arthritis. A murine autoimmune model of rheumatoid arthritis. Methods Mol Med. 2004; 102:313–38. [PubMed: 15286393]

12. Ohmura K, Johnsen A, Ortiz-Lopez A, Desany P, Roy M, Besse W, et al. Variation in IL-1beta gene expression is a major determinant of genetic differences in arthritis aggressivity in mice. Proc Natl Acad Sci U S A. 2005; 102:12489–94. [PubMed: 16113081]

13. Uysal H, Nandakumar KS, Kessel C, Haag S, Carlsen S, Burkhardt H, et al. Antibodies to citrullinated proteins: molecular interactions and arthritogenicity. Immunol Rev. 2010; 233:9–33. [PubMed: 20192990]

14. Koga T, Kakimoto K, Hirofuji T, Kotani S, Ohkuni H, Watanabe K, et al. Acute joint inflammation in mice after systemic injection of the cell wall, its peptidoglycan, and chemically defined peptidoglycan subunits from various bacteria. Infect Immun. 1985; 50:27–34. [PubMed: 3930403]

15. Horai R, Saijo S, Tanioka H, Nakae S, Sudo K, Okahara A, et al. Development of chronic inflammatory arthropathy resembling rheumatoid arthritis in interleukin 1 receptor antagonist-deficient mice. J Exp Med. 2000; 191:313–20. [PubMed: 10637275]

16. Sakaguchi N, Takahashi T, Hata H, Nomura T, Tagami T, Yamazaki S, et al. Altered thymic T-cell selection due to a mutation of the ZAP-70 gene causes autoimmune arthritis in mice. Nature. 2003; 426:454–60. [PubMed: 14647385]

17. Glant TT, Cs-Szabó G, Nagase H, Jacobs JJ, Mikecz K. Progressive polyarthritis induced in BALB/c mice by aggrecan from human osteoarthritic cartilage. Arthritis Rheum. 1998; 41:1007–18. [PubMed: 9627010]

18. Hanyecz A, Berlo SE, Szanto S, Broeren CPM, Mikecz K, Glant TT. Achievement of a synergistic adjuvant effect on arthritis induction by activation of innate immunity and forcing the immune response toward the Th1 phenotype. Arthritis Rheum. 2004; 50:1665–76. [PubMed: 15146438]

19. Glant TT, Buzas EI, Finnegan A, Negroiu G, Cs-Szabó G, Mikecz K. Critical role of glycosaminoglycan side chains of cartilage proteoglycan (aggrecan) in antigen recognition and presentation. J Immunol. 1998; 160:3812–9. [PubMed: 9558085]

20. Buzas E, Vegvari A, Murad YM, Finnegan A, Mikecz K, Glant TT. T-cell recognition of differentially tolerated epitopes of cartilage proteoglycan aggrecan in arthritis. Cell Immunol. 2005; 235:98–108. [PubMed: 16185673]

21. Szanto S, Bárdos T, Szabo Z, David CS, Buzás E, Mikecz K, et al. Induction of arthritis in HLA-DR4-humanized and HLA-DQ8-humanized mice by human cartilage proteoglycan aggrecan but only in the presence of an appropriate (non-MHC) genetic background. Arthritis Rheum. 2004; 50:1984–95. [PubMed: 15188376]

22. Zhang Y, Guerassimov A, Leroux J-Y, Cartman A, Webber C, Lalic R, et al. Arthritis induced by proteoglycan aggrecan G1 domain in BALB/c mice. Evidence for T cell involvement and the immunosuppressive influence of keratan sulfate on recognition of T and B cell epitopes. J Clin Invest. 1998; 101:1678–86. [PubMed: 9541498]

23. Murad YM, Szabo Z, Ludanyi K, Glant TT. Molecular manipulation with the arthritogenic epitopes of the G1 domain of human cartilage proteoglycan aggrecan. Clin Exp Immunol. 2005; 142:303–11. [PubMed: 16232217]

24. Glant TT, Bardos T, Vermes C, Chandrasekaran R, Valdéz JC, Otto JM, et al. Variations in susceptibility to proteoglycan-induced arthritis and spondylitis among C3H substrains of mice. Evidence of genetically acquired resistance to autoimmune disease. Arthritis Rheum. 2001; 44:682–92. [PubMed: 11263784]

25. Szabo Z, Szanto S, Vegvari A, Szekanecz Z, Mikecz K, Glant TT. Genetic control of experimental spondyloarthropathy. Arthritis Rheum. 2005; 52:2452–60. [PubMed: 16059927]

26. Finnegan A, Mikecz K, Tao P, Glant TT. Proteoglycan (aggrecan)-induced arthritis in BALB/c mice is a Th1-type disease regulated by Th2 cytokines. J Immunol. 1999; 163:5383–90. [PubMed: 10553063]

27. Hollo K, Glant TT, Garzo M, Finnegan A, Mikecz K, Buzas EI. Complex pattern of Th1 and Th2 activation with a preferential increase of autoreactive Th1 cells in BALB/c mice with proteoglycan (aggrecan)-induced arthritis. Clin Exp Immunol. 2000; 120:167–73. [PubMed: 10759779]

28. Doodes PD, Cao Y, Hamel KM, Wang Y, Farkas B, Iwakura Y, et al. Development of proteoglycan-induced arthritis is independent of IL-17. J Immunol. 2008; 181:329–37. [PubMed: 18566398]

29. Doodes PD, Cao Y, Hamel KM, Wang Y, Rodeghero RL, Mikecz K, et al. IFN-{gamma} Regulates the Requirement for IL-17 in Proteoglycan-Induced Arthritis. J Immunol. 2010; 184:1552–9. [PubMed: 20028652]

30. Boldizsar F, Tarjanyi O, Nemeth P, Mikecz K, Glant TT. Th1/Th17 polarization and acquisition of an arthritogenic phenotype in arthritis-susceptible BALB/c, but not in MHC-matched, arthritis-resistant DBA/2 mice. Int Immunol. 2009; 21:511–22. [PubMed: 19254958]

31. Ahlqvist E, Hultqvist M, Holmdahl R. The value of animal models in predicting genetic susceptibility to complex diseases such as rheumatoid arthritis. Arthritis Res Ther. 2009; 11:226–35. [PubMed: 19490601]

32. Cai C, La Cava A. Mimicking self-antigens with synthetic peptides in systemic autoimmune rheumatic diseases. Curr Clin Pharmacol. 2009; 4:142–7. [PubMed: 19442079]

33. van den Berg WB. Lessons from animal models of arthritis over the past decade. Arthritis Res Ther. 2009; 11:250. [PubMed: 19849822]

34. Taneja V, Taneja N, Paisansinsup T, Behrens M, Griffiths M, Luthra H, et al. CD4 and CD8 T cells in susceptibility/protection to collagen-induced arthritis in HLA-DQ8-transgenic mice: implications for rheumatoid arthritis. J Immunol. 2002; 168:5867–75. [PubMed: 12023391]

35. Taneja V, Behrens M, Mangalam A, Griffiths MM, Luthra HS, David CS. New humanized HLA-DR4-transgenic mice that mimic the sex bias of rheumatoid arthritis. Arthritis Rheum. 2007; 56:69–78. [PubMed: 17195209]

36. Taneja V, Behrens M, Basal E, Sparks J, Griffiths MM, Luthra H, et al. Delineating the role of the HLA-DR4 "shared epitope" in susceptibility versus resistance to develop arthritis. J Immunol. 2008; 181:2869–77. [PubMed: 18684978]

37. Kidd BA, Ho PP, Sharpe O, Zhao X, Tomooka BH, Kanter JL, et al. Epitope spreading to citrullinated antigens in mouse models of autoimmune arthritis and demyelination. Arthritis Res Ther. 2008; 10:R119. [PubMed: 18826638]

38. Jasin HE. Autoantibody specificities of immune complexes sequestered in articular cartilage of patients with rheumatoid arthritis and osteoarthritis. Arthritis Rheum. 1985; 28:241–8. [PubMed: 2983739]

39. Monach PA, Hueber W, Kessler B, Tomooka BH, Benbarak M, Simmons BP, et al. A broad screen for targets of immune complexes decorating arthritic joints highlights deposition of nucleosomes in rheumatoid arthritis. Proc Natl Acad Sci U S A. 2009; 106:15867–72. [PubMed: 19720992]

40. Stuart JM, Dixon FJ. Serum transfer of collagen-induced arthritis in mice. J Exp Med. 1983; 158:378–92. [PubMed: 6886622]

41. Korganow A-S, Ji H, Mangialaio S, Duchatelle V, Pelanda R, Martin T, et al. From systemic T cell self-reactivity to organ-specific autoimmune disease via immunoglobulins. Immunity. 1999; 10:451–61. [PubMed: 10229188]

42. Kuhn KA, Kulik L, Tomooka B, Braschler KJ, Arend WP, Robinson WH, et al. Antibodies against citrullinated proteins enhance tissue injury in experimental autoimmune arthritis. J Clin Invest. 2006; 116:961–73. [PubMed: 16585962]

43. Nielen MM, van Schaardenburg D, Reesink HW, Twisk JW, van de Stadt RJ, van der Horst-Bruinsma IE, et al. Simultaneous development of acute phase response and autoantibodies in preclinical rheumatoid arthritis. Ann Rheum Dis. 2006; 65:535–7. [PubMed: 16079166]

44. Goldbach-Mansky R, Lee J, McCoy A, Hoxworth J, Yarboro C, Smolen JS, et al. Rheumatoid arthritis associated autoantibodies in patients with synovitis of recent onset. Arthritis Res. 2000; 2:236–43. [PubMed: 11056669]

45. Andersson AK, Li C, Brennan FM. Recent developments in the immunobiology of rheumatoid arthritis. Arthritis Res Ther. 2008; 10:204–12. [PubMed: 18373887]

46. Aletaha D, Neogi T, Silman AJ, Funovits J, Felson DT, Bingham CO III, et al. rheumatoid arthritis classification criteria: an American College of Rheumatology/European League Against Rheumatism collaborative initiative. Ann Rheum Dis. 2010; 69:1580–8. (and A&R, 62:2569–2581). [PubMed: 20699241]

47. Cs-Szabó G, Roughley PJ, Plaas A, Glant TT. Large and small proteoglycans of osteoarthritic and rheumatoid articular cartilage. Arthritis Rheum. 1995; 38:660–8. [PubMed: 7538297]
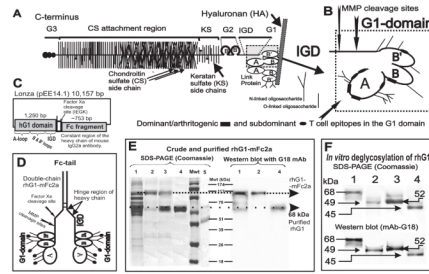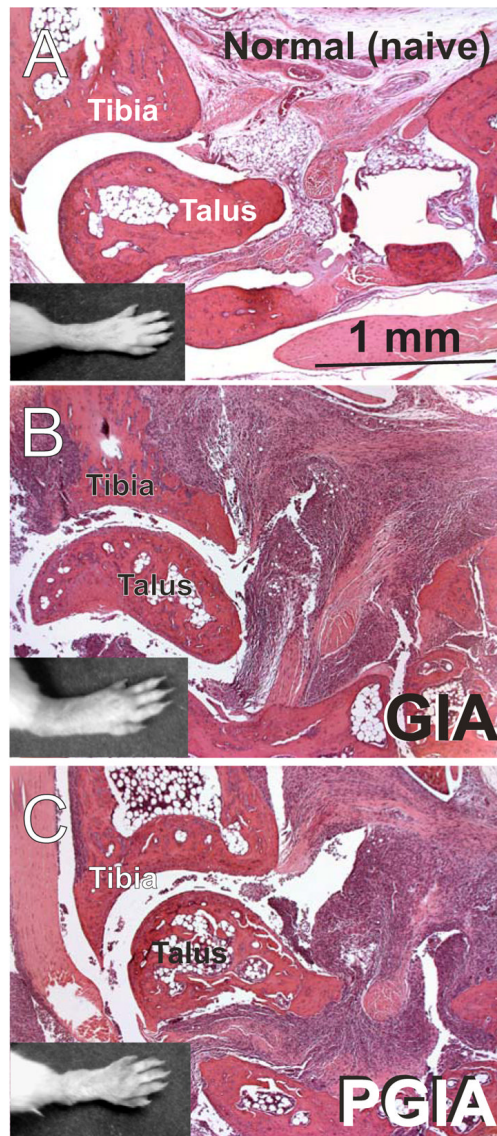
Figure 1.
Schematics of the cartilage proteoglycan (PG) aggrecan, G1 domain, the mammalian expression vector containing the rhG1 fusion construct, and the analysis of expressed recombinant proteins. **A,** The PG molecule consists of a protein core to which hundreds of glycosaminoglycan side chains (chondroitin sulfate [CS] or keratan sulfate [KS] are attached together with O-linked and N-linked oligosaccharides. The B and B' loops of the G1 domain of the aggrecan PG core protein (PG monomer) interact with hyaluronan (HA) in cartilage; this interaction is stabilized by link protein (LP). Core protein structure: G1, G2 and G3 are the globular domains; IGD is the interglobular domain; KS is the keratan sulfate-rich domain; CS is the chondroitin sulfate attachment region (this figure is an adaptation of figures from references (19) and (5)). **B,** Detailed structure of the G1 domain, including the major cleavage sites for stromelysin (MMP3) and two aggrecanases (ADAMTS-4 and ADAMTS-5). Three dominant/arthritogenic and four subdominant epitopes are located in the G1 domain (20,21). Thus, less than 0.02% of the molecular mass, or less than 15% of the core protein (i.e., the G1 domain), drives the arthritogenic response to PG in genetically susceptible BALB/c mice. **C,** The rhG1-Xa-mFc2a construct in a Lonza pEE14.1 mammalian expression vector. **D,** Schematics of the "double-chain" rhG1-mFc2a fusion protein. The C-terminal end of the heavy chain of mouse IgG2a (Fc tail) is linked, via the hinge region, to the G1 domain of PG. The heavy chains are able to reform the disulfide bridges. A properly folded Fc tail binds to Protein A or Protein G, thus allowing for purification by affinity chromatography. **E,** Detection of the rhG1-Xa-mFc2a protein, separated by 12% SDS-PAGE and stained with Coomassie Blue G-250 (left-hand panel) and separated by western blot and stained with mAb G18 (right–hand panel). Lane 1: unpurified CHO serum-free medium harvested from rhG1-Xa-mFc2a-transfected and cloned CHO cells (roughly 30 μg protein). Lane 2: Protein G-purified rhG1-Xa-mFc fusion protein from the same CHO-SFM (5 μg protein). Lane 3: purified rhG1-Xa-mFc2a fusion protein after cleavage with factor Xa. Lane 4: rhG1 protein re-purified using Protein G/Sepharose. Lane 5 contains highly purified native human G1 domain (~42 kDa) isolated from human cartilage PG as previously described (19). Molecular weight markers (Mwt) are indicated in kDa. **F,** *In vitro* de-glycosylation of rhG1 yields a lower molecular mass protein. Lane 1: purified rhG1 without Fc-tail. Lane 2: rhG1 digested with PNGase F (thus removing all *N*-linked oligosaccharides). Lane 3: rhG1 digested with keratanases 1 and 2. Lane 4: digested with all enzymes (PNGase F, keratanases, sialidase and O-glycosidase), thus removing both *N*-linked and *O*-linked oligosaccharides.
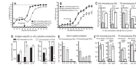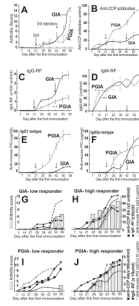
Figure 2.
Comparison of disease development and immune responses in mice with GIA and PGIA. **A,** Incidence and **B**, severity of arthritis in BALB/c mice immunized with either rhG1-Xa-mFc2a fusion protein (40 μg G1/injection) or cartilage PG (100 μg/injection) isolated from osteoarthritic cartilage (11,17,47). Vertical arrows indicate the third injection administered on day 42. Each animal was scored for arthritis three times a week, and the scores are shown as mean ± SEM. **C,** T-cell proliferation and IL-2 production in response to stimulation with rhG1 or PG. **D,** In vitro antigen (rhG1 and human PG)-induced cytokine production by spleen cells isolated from mice with GIA and PGIA, respectively. (**E**) Serum levels of cytokines and (**F**) anti-PG antibodies in mice with GIA and PGIA. The results shown in panels **C-F** are mean values ± SEM. Asterisks indicate statistically significant differences (*p < 0.05 and **p < 0.01).

Figure 3.
Macroscopic images of hind limbs (black and white inserts) and histopathology of corresponding ankle joints of a normal (non-immunized) mouse (**A**) and in mice with GIA (**B**) or PGIA (**C**). Sections of decalcified hind paws of mice were stained with hematoxylin and eosin. There were no clinically or histologically detectable differences when arthritic limbs were compared between animals immunized with rhG1-Xa-mFc2a or rhG1(GIA) and those immunized with human cartilage PG (PGIA). In contrast to the normal joint (**A**), ankles in GIA (**B**) and PGIA (**C**) showed histological evidence of inflammation, synovial pannus formation, and cartilage and bone destruction.

Figure 4.
Kinetics of autoantibody production in the context of arthritis development in GIA (rhG1-immunized) and PGIA. Arthritis scores (A), and serum levels of anti-cyclic citrullinated peptide (CCP) antibodies **(B)**, rheumatoid factors (IgG- and IgM-type RF) **(C, D)**, and autoantibodies to mouse cartilage PG (**E, F**) were monitored in rhG1- and PG-immunized mice between days 7 and 58 of immunization. Results from 17 mice with GIA and 14 mice with PGIA are shown. Panels **G-J** show individually analyzed arthritis scores and corresponding autoantibody titers in low and high responder mice in the GIA and PGIA groups. Although the results for only one low and one high responder mouse from each group are compared here, similar results were obtained in a replicate experiment. Note, the right *y*-axis scales in panels **G, H, I, J** are different from those shown in panels **B, C, E, F**.